Flow past a Cylinder on a β Plane, with Application to Gulf Stream Separation and the Antarctic Circumpolar Current

CLAIRE E. TANSLEY AND DAVID P. MARSHALL

Department of Meteorology, University of Reading, Reading, United Kingdom

(Manuscript received 1 May 2000, in final form 11 April 2001)

ABSTRACT

The classical problem of flow past a cylinder is revisited in the context of understanding two oceanographic phenomena: separation of the Gulf Stream from the North American coastline at Cape Hatteras and the interaction of the Antarctic Circumpolar Current with topographic obstacles. Numerical solutions are presented for eastward, barotropic flow past a cylinder in a β-plane channel. The solutions are dependent on two nondimensional parameters: the Reynolds number, Re, and a nondimensional β parameter, $\hat{\beta}$. In line with previous studies, increasing $\hat{\beta}$ reduces the separation downstream of the cylinder but introduces a blocked stagnant region upstream of the cylinder, flanked by two inertial jets. The large $\hat{\beta}$ limit is relevant to the interaction of the Antarctic Circumpolar Current with topographic obstacles such as the Kerguelen Plateau. However, a new regime is obtained for high Reynolds number (Re $>$ 200) and moderate β parameter ($\hat{\beta} \sim$ 10–100) with two separated jets *downstream* of the cylinder. These jets can extend a considerable distance, maintained by breaking Rossby waves in the turbulent wake of the cylinder, within which there is a downscale cascade of vorticity and an upscale cascade of energy toward the Rhines scale. Through a series of numerical experiments, the authors demonstrate the relevance of this regime to the separation of a boundary current from a cape. The implications are that Gulf Stream separation at Cape Hatteras is the consequence of *both* the high Reynolds number in the ocean and the moderate β parameter associated with the curvature of the coastline at Cape Hatteras. Results also suggest that geostrophic eddy fluxes are essential in maintaining a tight separated jet.

1. Introduction

Flow past a cylinder in a nonrotating fluid is the classical paradigm of flow separation, and is often cited in discussions of boundary current separation in the ocean (e.g., Dengg 1993). The separation behavior is controlled by the Reynolds number,

$$\mathrm{Re} = \frac{UL}{\nu}, \tag{1}$$

a measure of the ratio of inertia and viscous forces, where U and L are typical velocity and length scales, respectively, and ν is the viscosity. In the case of flow past a cylinder, U corresponds to the background velocity and L to the diameter of the cylinder. A beautiful series of photographs of the flow regimes obtained at different Reynolds numbers is presented in Van Dyke (1982). At low Reynolds number, Re $<$ 1, the flow is fairly symmetric upstream and downstream, and there is no separation. As the Reynolds number is increased to 10 $<$ Re $<$ 40, laminar separation is obtained with two steady vortices downstream of the cylinder. At moderate Reynolds numbers, 40 $<$ Re $<$ 10^3, the steady vortices are replaced by a periodic ''von Kármán vortex street,'' and finally for Re $>$ 10^3, the separated flow becomes increasingly turbulent.

The Reynolds number in the ocean is extremely large. For example, in the Gulf Stream, taking $U \sim 0.1$ m s^{-1}, $L \sim 10^5$ m, and $\nu \sim 10^{-6}$ m^2 s^{-1} gives Re $\sim 10^{10}$, which would suggest that the Gulf Stream is always liable to separate from the North American coastline. In contrast in a coarse-resolution ocean model, a typical viscosity is $\nu \sim 10^3$ m^2 s^{-1}, giving a Reynolds number of only Re $\sim$ 10. The inability of ocean models to simulate the separation of boundary currents, such as the Gulf Stream, is therefore often attributed to the spurious low Reynolds numbers in such models (e.g., Dengg 1993).

However, these arguments are incomplete to the extent that the separation behavior of fluid flows is significantly modified by differential rotation. The properties of flow past a cylinder on a β plane have been discussed in a series of papers in the fluid mechanics literature. Briefly, the β effect has been shown to inhibit separation in eastward flows (Merkine 1980; Boyer and Davies 1982; Foster 1985; Page and Johnson 1990), and in some cases, to produce an upstream region of blocked, stagnant flow (Foster 1985; Page and Johnson 1990).

Corresponding author address: Dr. David Marshall, Department of Meteorology, University of Reading, P.O. Box 243, Reading RG6 6BB, United Kingdom.
E-mail: d.p.marshall@reading.ac.uk

In this manuscript, our aims are (i) to introduce the characteristics of flow separation on a β plane to the oceanographic literature; (ii) to extend some of the results for flow past a cylinder to new parameter regimes; and (iii) to relate these results to two oceanographic phenomena, namely Gulf Stream separation and the interaction of the Antarctic Circumpolar Current with topographic obstacles such as the Kerguelen Plateau. The key nondimensional parameters are defined in section 2, numerical solutions are presented in section 3, the application of these solutions to Gulf Stream separation and Southern Ocean jets is discussed in section 4, and concluding remarks are given in section 5.

2. Nondimensional parameters

We consider barotropic eastward flow in a channel of constant depth on a β plane. The Coriolis parameter is given by $f = f_0 + \beta y$, where f_0 and β are constants. The barotropic vorticity equation can be written

$$\frac{\partial \zeta}{\partial t} + \mathbf{u} \cdot \nabla(\zeta + \beta y) = \nu \nabla^2 \zeta, \tag{2}$$

where $\mathbf{u}$ is the fluid velocity, ζ is the relative vorticity, and ν is the kinematic viscosity of the fluid. Defining a characteristic length scale L and a characteristic velocity scale U, we nondimensionalize the vorticity equation by defining nondimensional variables $(\tilde{x}, \tilde{y}) = (x, y)/L$, $\tilde{\mathbf{u}} = \mathbf{u}/U$, $\tilde{\zeta} = \zeta L/U$, $\tilde{t} = tU/L$, such that (2) becomes

$$\frac{\partial \tilde{\zeta}}{\partial \tilde{t}} + \tilde{\mathbf{u}} \cdot \tilde{\nabla} \tilde{\zeta} + \hat{\beta} \tilde{v} = \frac{\tilde{\nabla}^2 \tilde{\zeta}}{\mathrm{Re}}. \tag{3}$$

Here Re is the Reynolds number as defined in (1), and

$$\hat{\beta} = \frac{\beta L^2}{U} = \left(\frac{L}{L_R}\right)^2 \tag{4}$$

is a nondimensional ''β parameter,'' where $L_R = (U/\beta)^{1/2}$ is the ''Rhines scale'' (Rhines 1975). There are several possible interpretations of $\hat{\beta}$, but perhaps the most helpful is as quantifying the extent to which fluid parcels are confined meridionally. Over meridional scales less than the Rhines scale ($\hat{\beta} < 1$), fluid parcels are relatively free to move around, and the flow can often be characterized as turbulent. However, on scales greater than the Rhines scale ($\hat{\beta} > 1$), the β effect exerts a strong restoring force, and the flow patterns organize themselves into Rossby waves. This process provides a barrier to the upscale cascade of energy in geostrophic turbulence, and consequently there is a tendency for turbulent rotating flows to evolve toward a series of zonal jets separated by the Rhines scale (Rhines 1975; Williams 1978).

In the remainder of this paper, our results are presented in terms of the two nondimensional parameters, Re and $\hat{\beta}$. However, there is a complimentary nondimensionalization of the vorticity equation that relates more directly to ocean gyre theory (e.g., Pedlosky 1987). In this instance the terms are scaled relative to the advection of planetary, rather than relative vorticity. Thus, dividing (3) by $\hat{\beta}$ we obtain

$$\frac{1}{\hat{\beta}}\left(\frac{\partial \tilde{\zeta}}{\partial \tilde{t}} + \tilde{\mathbf{u}} \cdot \tilde{\nabla} \tilde{\zeta}\right) + \tilde{v} = \frac{1}{\hat{\beta}\mathrm{Re}} \tilde{\nabla}^2 \tilde{\zeta}, \tag{5}$$

where

$$\frac{1}{\hat{\beta}} = \left(\frac{\delta_I}{L}\right)^2 \quad \text{and} \tag{6}$$

$$\frac{1}{\hat{\beta}\mathrm{Re}} = \left(\frac{\delta_M}{L}\right)^3. \tag{7}$$

Here $\delta_I = (U/\beta)^{1/2}$ is the width of an inertial boundary layer (Fofonoff 1954; note $\delta_I = L_R$) and $\delta_M = (\nu/\beta)^{1/3}$ is the width of a frictional boundary layer (Munk 1950). Strictly, a confined inertial boundary current can only form if the background flow is westward; in background eastward flow, inertia and friction combine to give a damped stationary Rossby wave of wavelength $2\pi\delta_I$ that decays away from a western boundary (Moore 1963). Nevertheless, varying $\hat{\beta}$ and Re is equivalent to varying the relative importance of inertia and viscosity in any boundary layers attached to the cylinder, and the width of these boundary layers relative to the diameter of the cylinder.

Note that the absolute value of the Coriolis parameter, f_0, does not enter into the barotropic vorticity equation. However, in laboratory experiments (Boyer 1970) and certain numerical and analytical studies (e.g., Merkine and Solan 1979), Ekman layers are introduced at the top and bottom of the channel. Ekman pumping provides an alternative and more efficient mechanism of vorticity dissipation than viscosity alone. Since the Ekman pumping depends on the value of f_0, the behavior of flows past a cylinder is dependent on the Rossby number in the presence of Ekman layers. However, in the ocean there is no rigid surface boundary, suggesting that a surface Ekman layer in order to satisfy a no-slip boundary condition is inappropriate. Moreover, since currents are generally surface intensified, introducing a bottom Ekman layer into a barotropic model is likely to overstate the influence of the bottom boundary on such currents. In this study, therefore, we do not consider Ekman layers and our solutions are independent of the Rossby number.

3. Numerical results

We now present a series of numerical solutions for flow past a cylinder in a periodic zonal channel. A schematic of the model domain is shown in Fig. 1. The length of the channel is $16L$ and its width is $4L$. One of the issues in modeling such flows on a β plane is whether it is appropriate to apply either an upstream or down-

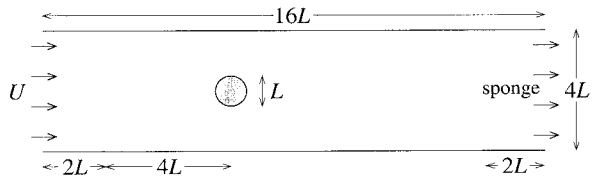

FIG. 1. A schematic of the model domain, consisting of a cylinder of diameter L within a periodic zonal channel of dimensions $16L \times 4L$. Within the shaded sponge layer, the zonal velocity is relaxed toward a uniform value, U.

stream boundary condition. For example, previous studies have shown that the westward propagation of Rossby waves introduces a downstream control in the limit of finite $\hat{\beta}$ (Boyer and Davies 1982; Foster 1985; Page and Johnson 1990), whereas one would expect to revert to the classical upstream control in the limit of $\hat{\beta} \to 0$. Here we sidestep this issue by relaxing the zonal velocity toward a uniform eastward flow, speed U, within a sponge region of zonal extent $4L$. The relaxation coefficient varies smoothly between zero outside the sponge and a maximum value within the central half of the sponge; the maximum relaxation coefficient is varied between solutions to account for the different wave propagation speeds. The sponge prevents disturbances from propagating all the way around the channel, but also enables the solution to select the appropriate boundary condition (upstream, downstream, or some combination of both). The cylinder, of diameter L, is placed a distance $4L$ downstream of the sponge.

The solutions are obtained by numerically integrating the barotropic vorticity equation to a statistically steady state on a grid of 512×128 points, giving a spatial resolution of $L/32$. Standard finite difference methods are employed. The advection term is differenced using the energy- and enstrophy-conserving Arakawa Jacobian. Time stepping is by a leapfrog scheme with a Robert–Aselin filter applied to prevent adjacent time steps from diverging; the viscous and relaxation terms are backward differenced in time. A multigrid inverter is used to invert the vorticity field for the streamfunction. Boundary conditions are no normal flow and no slip on the walls of the cylinder, represented in a piecewise-constant manner. The piecewise-constant approximation is adopted both for convenience and for consistency with the vast majority of ocean general circulation models; however note the cautionary comments of Adcroft and Marshall (1998). On the sidewall of the channel we apply no-normal-flow and free-slip boundary conditions, the latter chosen in order to minimize any impact on the interior flow. The value of the streamfunction on the wall of the cylinder is determined by ensuring that there is no net torque acting on the cylinder.

a. f PLANE

We first consider a constant Coriolis parameter (i.e., $\hat{\beta} = 0$). The solutions correspond to those obtained in a nonrotating frame (e.g., Batchelor 1967; Van Dyke 1982) since the absolute value of the Coriolis parameter does not enter into the barotropic vorticity equation (3). For each solution we show snapshots of the streamfunction (ψ, defined such that $\tilde{\mathbf{u}} = \mathbf{k} \times \nabla\psi$) and the vorticity ($q = \tilde{\zeta} + \hat{\beta}\tilde{y}$).

A series of three solutions at different Reynolds numbers are shown in Fig. 2. First, at Re = 1 (Fig. 2a), the flow is steady and nearly symmetric upstream and downstream of the cylinder. There is no separation, but a closer inspection reveals slightly enhanced deflection of

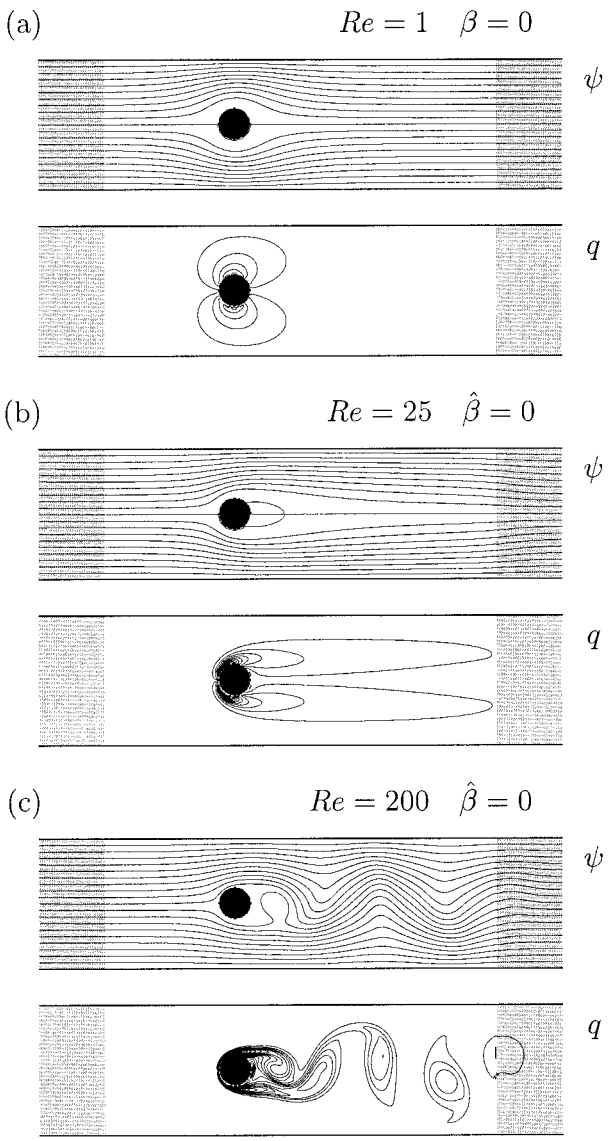

FIG. 2. Streamfunction (ψ) and vorticity (q) fields from solutions with constant Coriolis parameter ($\hat{\beta} = 0$) and Reynolds numbers of (a) Re = 1, (b) Re = 25, (c) Re = 200. Cases (a) and (b) are steady, whereas (c) settles into a periodic limit cycle. In this and subsequent figures the fields shown are snapshots unless indicated otherwise. The sponge layer is indicated by shading (note that the domain is periodic). Contour intervals are 0.2 for ψ and 1.0 for q in each case.

the streamlines downstream of the cylinder, associated with weak advection of the boundary vorticity anomalies by the background flow. At Re = 25 (Fig. 2b), the boundary vorticity anomalies are advected farther downstream, leading to separation and an enclosed region in which there are two weak recirculating eddies. As the Reynolds number increases the area of the downstream separated region increases and reaches a maximum at Re $\approx$ 50 (not shown); this compares favorably with the equivalent solution obtained at Re $\approx$ 41 in the classical nonrotating limit within an infinite domain. At Re $>$ 50, the flow is unsteady with counterrotating eddies being shed periodically downstream of the cylinder to form a von Kármán vortex street (Fig. 2c).

b. β *plane*

We now allow the Coriolis parameter to vary linearly in the meridional direction. In Fig. 3 we first consider a relatively low Reynolds number. For small values of $\hat{\beta}$ (Fig. 3a) there is little change from the f-plane case (Fig. 2b). This is to be expected since the wavelength of the standing Rossby waves ($2\pi\delta_I$) is larger than the width of the channel ($4L$). As $\hat{\beta}$ increases, upstream Rossby waves become apparent (White 1971). Figure 3b shows the flow for a value of $\hat{\beta} = 7.5$. The wavelength of the standing Rossby waves in this case corresponds to approximately $2L$. As the value of $\hat{\beta}$ is increased further (Fig. 3c), the wavelength of the downstream Rossby waves decreases and a western boundary current appears on the downstream face of the cylinder. The flow now fails to separate. There is direct analogy (e.g., Page and Johnson 1990) between these solutions and Long's model for stratified flow over a hill (Long 1955).

In some numerical calculations with negligible Ekman pumping, Merkine (1980) showed that the presence of β shifts the region of adverse pressure gradient downstream, and thus inhibits flow separation. For a value of $\hat{\beta} = 1$, the adverse pressure gradient shifts by approximately 20°, while for $\hat{\beta} = 4$ there is a 45° shift. The tendency of the β effect to suppress adverse pressure gradients has also been demonstrated analytically by Marshall and Tansley (2001). The suppression of the adverse pressure gradient can been seen in the numerical solutions through the bunching of streamlines on the downstream face of the cylinder as $\hat{\beta}$ increases, indicating acceleration rather than deceleration of the boundary layer flow.

At the same time, a stagnant, blocked region appears upstream for high values of $\hat{\beta}$. A similar blocking effect was found in both linear analysis and laboratory experiments by Hide and Hocking (1979). Page and Johnson (1990) describe how this region is formed by propagation of Rossby waves away from the cylinder so that eventually steady Rossby waves with a negative group velocity exactly balance the oncoming flow in the blocked region. Foster (1985) shows that the only steady-state solution for this upstream region is one of no flow. This is consistent with ocean gyre theory in which stable boundary currents are able to form only on the western margins of basins (e.g., Pedlosky 1987).

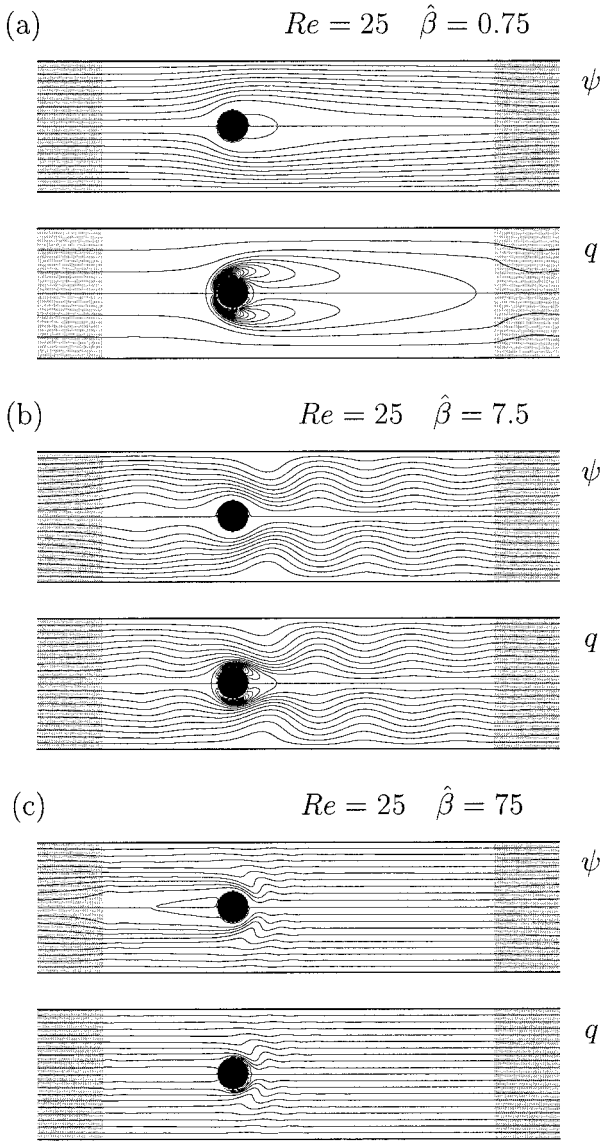

FIG. 3. Streamfunction (ψ) and vorticity (q) fields at Re = 25 and (a) $\hat{\beta} = 0.75$, (b) $\hat{\beta} = 7.5$, (c) $\hat{\beta} = 75$. Contour intervals are 0.2 for ψ and 0.5, 1.5, and 15 for q in (a), (b), and (c) respectively. Each of the solutions are steady.

In Fig. 4 we show the equivalent results for a larger Reynolds number, Re = 200. At the lowest value of $\hat{\beta} = 0.75$ the flow remains similar to the nonrotating case, with counterrotating vortices shed periodically downstream of the cylinder (Fig. 4a). At a moderate value of $\hat{\beta} = 7.5$, the downstream convergence of streamlines is more pronounced compared with the lower Reynolds number case. Two meandering jets form downstream of the cylinder, with a small separated region in between (Fig. 4b). Finally, in the case in which

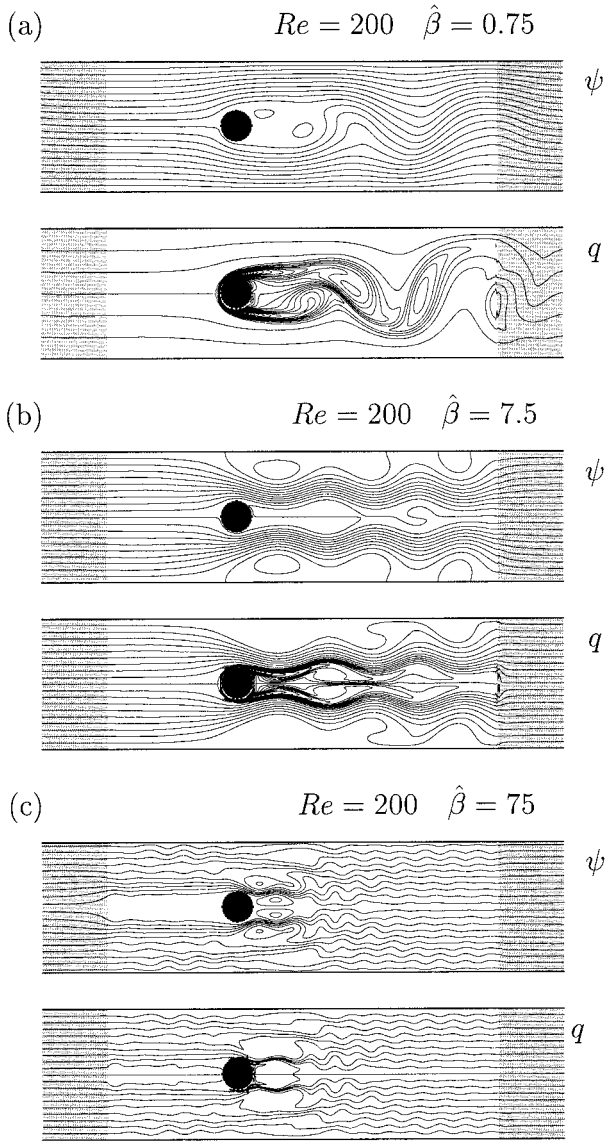

FIG. 4. Streamfunction (ψ) and vorticity (q) fields at Re = 200 and (a) $\hat{\beta} = 0.75$, (b) $\hat{\beta} = 7.5$, (c) $\hat{\beta} = 75$. Contour intervals are 0.2 for ψ and 0.5, 1.5, and 15 for q in (a), (b), and (c) respectively. Case (a) settles into a periodic limit cycle, whereas (b) and (c) are steady.

$\hat{\beta} = 75$, two intense separated jets again form downstream of the cylinder. Compared with the previous case, the jets are narrower and hence penetrate a shorter distance due to the enhanced dissipation (Fig. 4c). In both of the above cases the flow fields are steady, indicating that these jets are generated by separation of the boundary layer rather than through turbulent processes.

c. Higher Reynolds number

In our model there is an upper limit to the size of the Reynolds number we can achieve, set by the requirements of numerical stability. (The details of what sets this upper limit are complex, depending on the relative importance of advection and the β effect.) One solution to this problem is to introduce biharmonic dissipation, as is often done in high-resolution ocean general circulation models. The nondimensional barotropic vorticity equation (3) becomes

$$\frac{\partial \tilde{\zeta}}{\partial \tilde{t}} + \tilde{\mathbf{u}} \cdot \tilde{\boldsymbol{\nabla}} \tilde{\zeta} + \hat{\beta} \tilde{v} = \frac{\tilde{\nabla}^2 \tilde{\zeta}}{\mathrm{Re}} - \frac{\tilde{\nabla}^4 \tilde{\zeta}}{R_4}, \tag{8}$$

where

$$R_4 = \frac{UL^3}{K} \tag{9}$$

is an ''effective Reynolds number'' associated with the biharmonic dissipation and K is a biharmonic dissipation coefficient. At large scales R_4 is very large, whereas at the scale of the model grid R_4 is typically $O(1)$, indicating that the biharmonic dissipation is efficient at dissipating grid-scale structures that are inadequately resolved by the model, while leaving larger-scale structures alone.

In Fig. 5a we show a solution in which biharmonic dissipation ($R_4 = 3 \times 10^5$) is added to the case shown in Fig. 4c. The downstream separated jets are still very clear, but the effect of introducing the biharmonic dissipation is to slightly reduce their zonal extent, as would be expected. In Fig. 5b we show a solution in which the Reynolds number is increased to 500. The penetration of the jets downstream of the cylinder is vastly increased compared with the previous case. Finally, in Fig. 5c the Reynolds number is increased further to 1000, resulting in jets that virtually extend across to the sponge. Also note the presence of secondary jets to the north and south of the cylinder. The structure of these jets is clearer in the mean streamfunction field (Fig. 6), which indicates a transition from four to six jets a distance $4L$ downstream of the cylinder.

While the central jets are initially formed through separation of the boundary layer, the mechanism responsible for their extension, and for the existence of the secondary jets, is similar to the organization of freely decaying turbulence described by Rhines (1975). At higher Reynolds number, the Rossby waves break downstream of the cylinder to form a geostrophic turbulent wake, evident from the filamentation in the vorticity fields in Figs. 5b and 5c. In geostrophic turbulence there is a direct cascade of vorticity to small spatial scales, but an inverse cascade of energy that is arrested in the meridional wavenumber at the Rhines scale. Consequently, energy accumulates at the Rhines scale, resulting in a series of zonal jets. The role of eddies in maintaining the jets is confirmed in Fig. 7, in which we show the first two terms on the right-hand side of the time-mean vorticity equation,

$$\frac{\partial \overline{\zeta}}{\partial t} + \overline{\mathbf{u}} \cdot \boldsymbol{\nabla} \overline{\zeta} + \hat{\beta} \overline{v} = -\boldsymbol{\nabla} \cdot \overline{\zeta' \mathbf{u}'} + \frac{\nabla^2 \overline{\zeta}}{\mathrm{Re}} - \frac{\nabla^4 \overline{\zeta}}{R_4}. \tag{10}$$

Here overbars and primes denote mean and transient

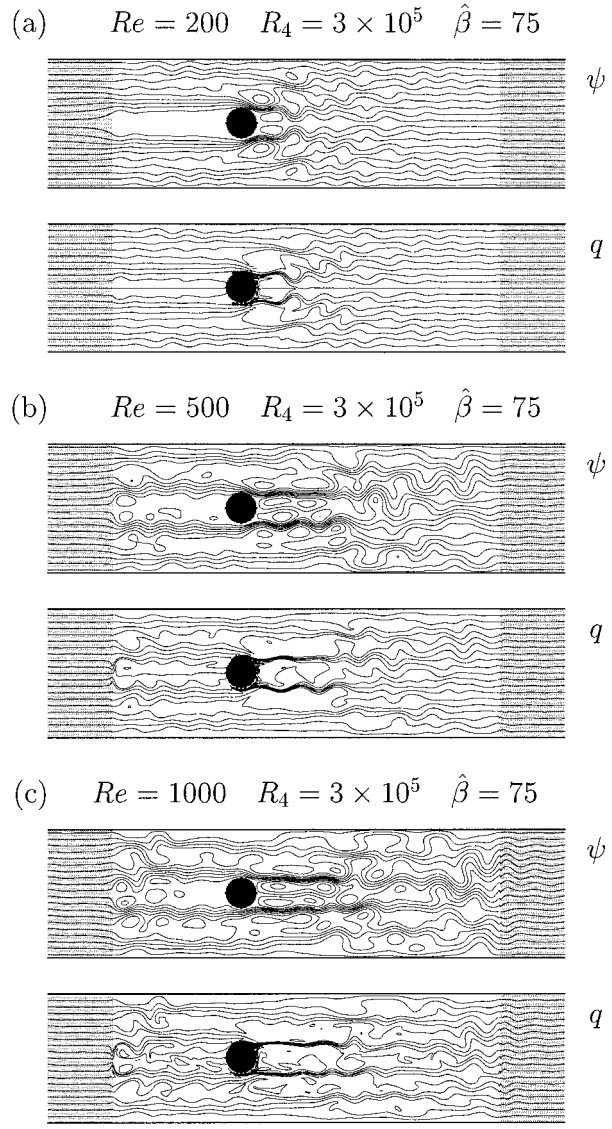

FIG. 5. Snapshots of the streamfunction (ψ) and vorticity (q) fields at $\hat{\beta} = 75$ and (a) Re = 200, (b) Re = 500, (c) Re = 1000. A small amount of biharmonic dissipation has been added to maintain numerical stability ($R_4 = 3 \times 10^5$). Contour intervals are 0.2 for ψ and 15 for q in each case. Solution (a) is steady, whereas solutions (b) and (c) produce a turbulent wake.

components respectively, and tildes have been dropped in the interests of clarity. The eddy vorticity flux convergence (Fig. 7a) contains a complex structure in the wake of the cylinder, but there is a clear tendency for the eddies to add vorticity to the north of the jets (unshaded contours) and to remove vorticity south of the jets (shaded contours); this pattern is consistent with acceleration of the mean flow. In contrast the effect of the viscous term (Fig. 7b) is the opposite; that is, it decelerates the mean flow. The dominant balance is between these two terms and the advection of vorticity by the mean flow, with the biharmonic dissipation being of secondary importance.

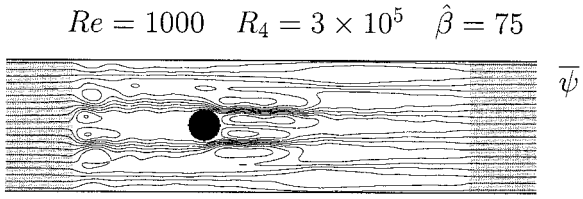

FIG. 6. Time-mean streamfunction field from the solution with $\hat{\beta} = 75$ and Re = 1000. The contour interval is 0.2.

In section 4 we will demonstrate that the generation of these inertial jets has important implications for understanding and modeling the separated Gulf Stream.

d. Larger $\hat{\beta}$

With the addition of a small amount of biharmonic dissipation, we can also explore solutions with larger values of $\hat{\beta}$, corresponding to a smaller Rhines scale. In Fig. 8, we show a series of solutions in which $\hat{\beta}$ is increased to 750, resulting in further inhibition of separation downstream of the cylinder. For a Reynolds number of 25, the flow does not separate (Fig. 8a). For a higher Reynolds number of 200, vortices form at the ''shoulders'' of the cylinder and the flow momentarily

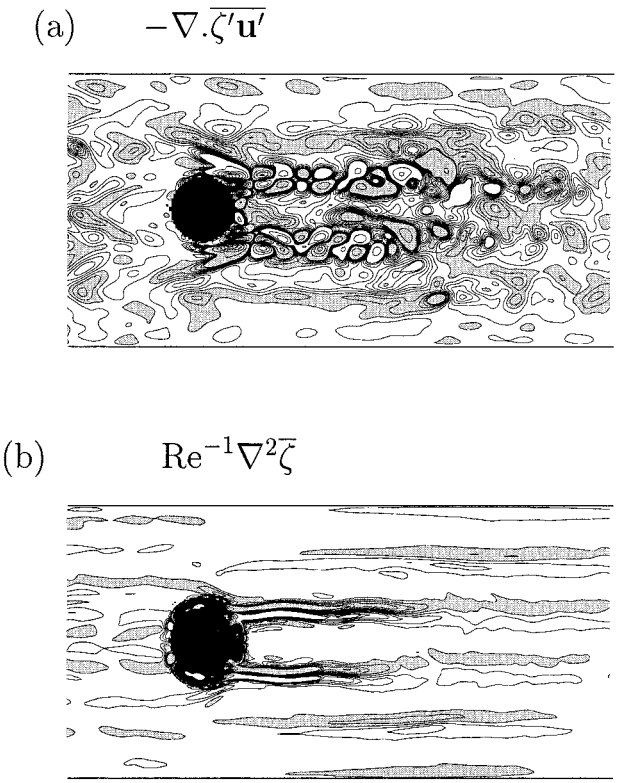

FIG. 7. (a) Time-mean eddy vorticity flux convergence and (b) mean viscous dissipation from the solution with Re = 1000 and $\hat{\beta} = 75$. Only the central portion of the channel is shown. The contour interval is 1.0 between values of -4.5 and 4.5, and 10.0 for larger values. Negative contours are shaded; the zero contour is not plotted.

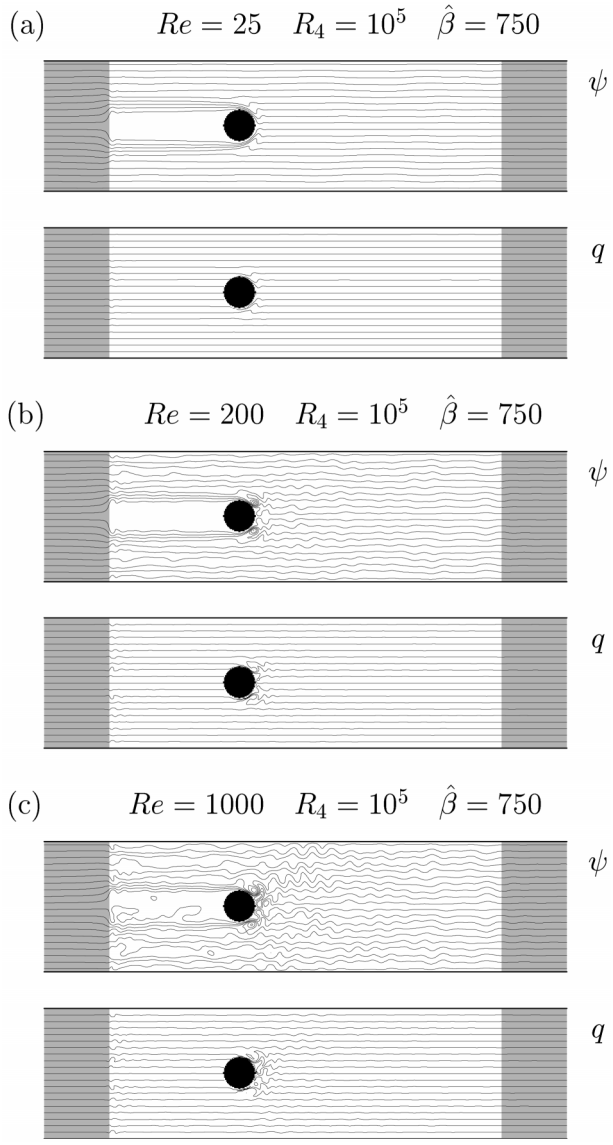

FIG. 8. Streamfunction (ψ) and vorticity (q) fields at $\hat{\beta} = 750$ and (a) Re = 25, (b) Re = 200, (c) Re = 1000. A small amount of biharmonic dissipation has been added to maintain numerical stability ($R_4 = 10^5$). Contour intervals are 0.2 for ψ and 150 for q in each case. The far-field Rossby waves visible in the solutions are eastward propagating and largely disappear in the time-mean fields.

separates but then reattaches (Fig. 8b). If we increase the Reynolds number further to 1000, the small-wavelength Rossby waves fill the channel (Fig. 8c). The finite model resolution prevents us from decreasing the dissipation to the point that wave breaking can occur in these solutions. If the model resolution were increased and the dissipation appropriately reduced, we anticipate that Rhines jets might be obtained downstream of the cylinder, as in Fig. 5, although the number of jets would be increased due to the larger $\hat{\beta}$. It is unclear whether the formation of such jets would modify our conclusions concerning the inhibition of separation at large $\hat{\beta}$; this issue requires further study.

e. Summary

To summarize, the key results of relevance to the ocean are the following.

- In order for an eastward current to separate downstream of an obstacle, it is necessary to have *both* a sufficiently large Reynolds number and a moderate β parameter. At higher Reynolds numbers, the Rossby waves break downstream of the cylinder, leading to the formation of separated, inertial jets.
- For larger values of $\hat{\beta}$, a stagnant region forms upstream of the obstacle, flanked by two inertial jets, and separation is inhibited downstream.

These results suggest two clear applications, to the separation of boundary currents such as the Gulf Stream and to the interaction of the Antarctic Circumpolar Current with topographic features.

4. Applications

a. Gulf Stream separation

A perennial problem with ocean general circulation models is the failure of model boundary currents to separate from coastlines. In particular, models have great difficulty in simulating the separation of the Gulf Stream from the North American coastline at Cape Hatteras [for a review, see Dengg et al. (1996)]. Nevertheless, the most recent simulations at 0.1° or higher lateral resolution show improved separation behavior (Paiva et al. 1999; Smith et al. 2000). To demonstrate the application of our results to Gulf Stream separation, we modify the model domain to include a quarter cylinder with straight boundaries upstream and downstream (Fig. 9), mimicking the geometry of the North American coastline at Cape Hatteras.

We first consider the problem directly analogous to the cylinder calculations in which a uniform flow is prescribed across the sponge layer. Here the Reynolds number and β parameter are defined using the relaxation velocity within the eastern sponge, and the diameter of the equivalent cylinder. These conventions allow direct comparison between the solutions and earlier results.

In Fig. 9a we show a solution with a moderate Reynolds number (Re = 100) and a high β parameter ($\hat{\beta} = 750$), similar parameters as in Fig. 8. There is a broad similarity between the two solutions, except that the Rossby waves are damped to a slightly greater extent in the present case, most likely due to the stabilizing influence of the solid coastline boundary. The flow completely fails to separate. In Fig. 9b we show the solution in which the β parameter is reduced by an order of magnitude (Re = 100, $\hat{\beta} = 75$). The boundary flow forms a broad jet, that initially separates but quickly

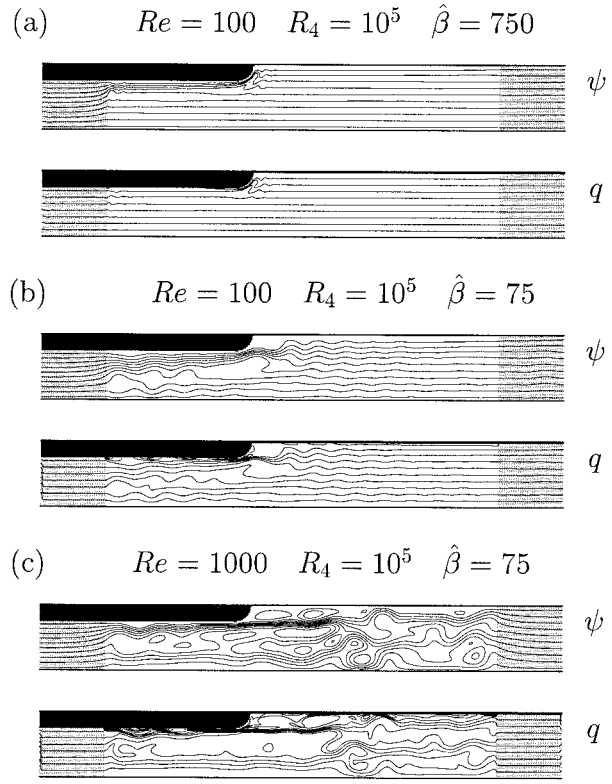

FIG. 9. Streamfunction (ψ) and vorticity (q) fields for flow along a coastline with a cape, mimicking Cape Hatteras: (a) Re = 100, $R_4 = 10^5$, $\hat{\beta} = 750$; (b) Re = 100, $R_4 = 10^5$, $\hat{\beta} = 75$; (c) Re = 1000, $R_4 = 10^5$, $\hat{\beta} = 75$. The velocity is relaxed to a uniform value within the sponges, but the domain is not periodic. Contour intervals are 0.2 for ψ in all cases, and 150 for q in case (a) and 15 for q in cases (b) and (c).

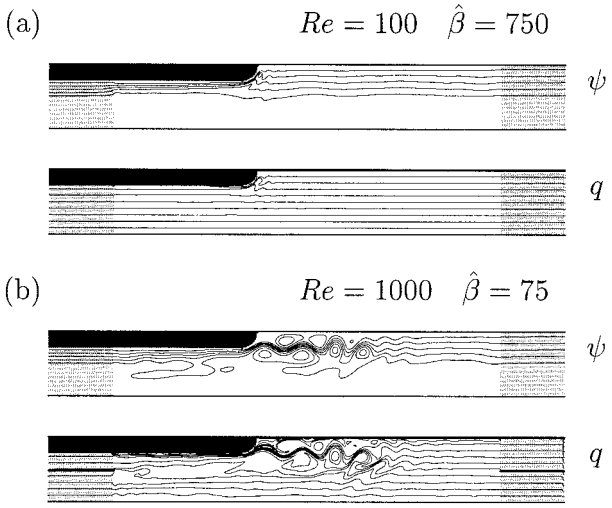

FIG. 10. Streamfunction (ψ) and vorticity (q) fields for a boundary current flowing along the same coastline as in Fig. 9: (a) Re = 100, $R_4 = 10^5$, $\hat{\beta} = 750$; (b) Re = 1000, $R_4 = 10^5$, $\hat{\beta} = 75$. Contour intervals are 0.2 for ψ in both cases, and 150 for q in case (a) and 15 for q in case (b).

diffuses into a broad flow and reattaches to the coastline. There is some similarity with the solution in Fig. 5a, but with reduced Rossby wave activity due to the slightly lower Reynolds number and the influence of the coastline. Finally, in Fig. 9c, we additionally increase the Reynolds number by an order of magnitude (Re = 1000, $\hat{\beta} = 75$). Now a tighter jet forms adjacent to the boundary and separates cleanly. The separated jet penetrates a considerable distance downstream, although not as far as in the corresponding cylinder solution (Fig. 5c). There is a weak recirculation gyre to the north of the separated jet, somewhat reminiscent of that found north of the separated Gulf Stream. The filamentation in the vorticity field again emphasizes the importance of eddies in maintaining the separated jet. An analysis of the eddy vorticity flux convergence confirms that the eddy term is $O(1)$ in the time-mean vorticity balance (not shown).

Finally, we illustrate the application of these results to boundary current separation by relaxing to a uniform flow only within the northern half of the channel. The nondimensional parameters are again evaluated using the relaxation velocity within the eastern sponge.

First, in Fig. 10a, with a low Reynolds number and high β parameter (Re = 100, $\hat{\beta} = 750$), the flow fails to separate and a damped Rossby wave forms against the cape, in a similar manner to the modeled Gulf Stream in many low-resolution ocean models [e.g., the 0.28° resolution experiment shown in Smith et al. (2000, Fig. 4b)]. In Fig. 10b we show the equivalent experiment with a larger Reynolds number and lower β parameter (Re = 1000, $\hat{\beta} = 75$). Here the boundary current separates and meanders propagate downstream, in a similar manner to observations of the Gulf Stream and the highest-resolution numerical simulations [e.g., the 0.1° resolution experiment shown in Smith et al. (2000, Fig. 4a)]. Filamentation in the vorticity field again indicates that eddies are active in the vorticity budget of the separated boundary current (not shown).

In comparison for the Gulf Stream, we estimate the following parameters: $\beta \sim 2 \times 10^{-11}$ m^{-1} s^{-1}, a radius of curvature in the coastline at Cape Hatteras of $L/2 \sim 2.5 \times 10^5$ m and $U \sim 10^{-1}$ m s^{-1} (note that the velocity of the separated boundary current is an order of magnitude greater than the relaxation velocity used to evaluate $\hat{\beta}$ in Fig. 10b). These parameters give $\hat{\beta} \sim 50$, a value that is most consistent with the separated solution in Fig. 10.

The above experiments emphasize the importance of achieving *both* a moderate β parameter ($\hat{\beta} \sim 10$–100) and a sufficiently high Reynolds number (Re > 200) for a boundary current to separate. The role of the geostrophic turbulent cascades in forming the downstream separated jets in these calculations also points to an important role for geostrophic eddy fluxes in maintaining the separated Gulf Stream.

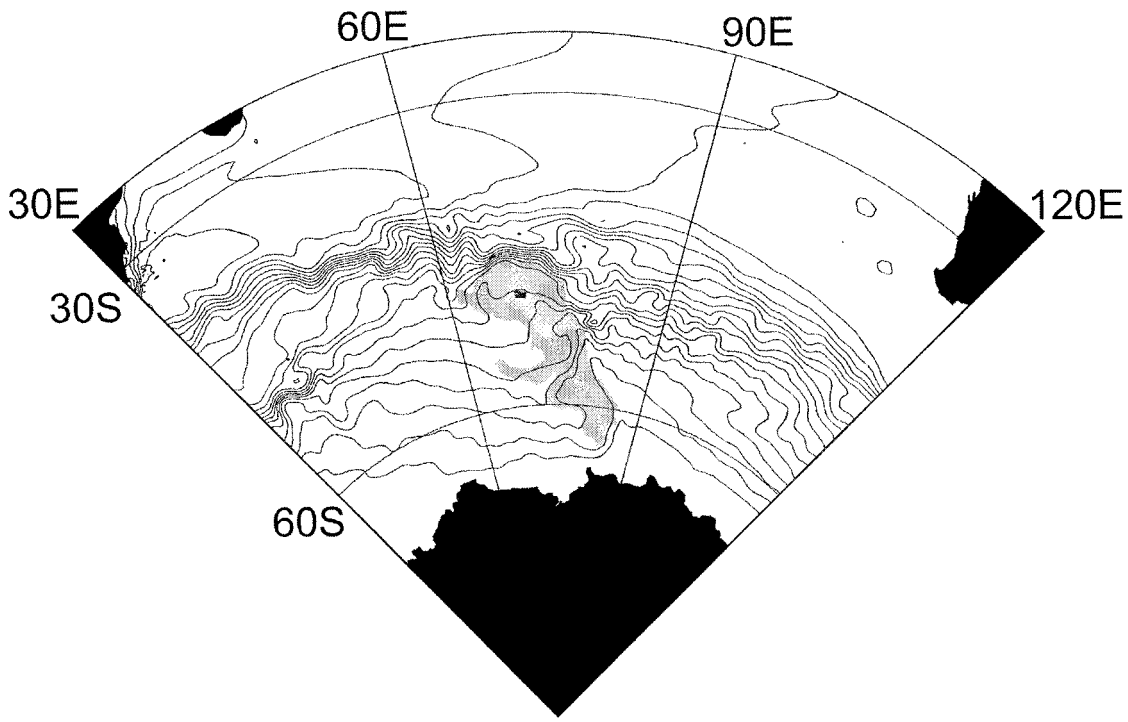

FIG. 11. Pressure field at 120 m from the FRAM simulation (contour interval: 10^3 Pa). The shading indicates the location of the 500- and 1000-m isobaths around the Kerguelen Plateau. [Adapted from Webb et al. (1991).]

b. Antarctic Circumpolar Current

For a higher value of $\hat{\beta}$, our results are relevant to the Antarctic Circumpolar Current, and in particular its interaction with topographic obstacles such as the Kerguelen Plateau. In Fig. 11 we reproduce a portion of the pressure field at 120 m from the Fine Resolution Antarctic Model (FRAM) simulation (Webb et al. 1991). These pressure contours are streamlines for the geostrophic flow. Upstream of the plateau there is a clear bunching of pressure contours into an inertial jet, whereas downstream of the plateau the pressure contours remain attached to the obstacle and feed into a series of standing Rossby waves.

Using the FRAM data we can estimate a typical Reynolds number and a β parameter. For consistency with our cylinder calculations, we identify the length scale with the north–south extent of the Kerguelen Plateau giving $L \sim 1.5 \times 10^6$ m, and using geostrophic balance we estimate a mean zonal velocity of $U \sim 0.1$ m s^{-1}. At the latitude of the plateau we have $\beta \sim 1.5 \times 10^{-11}$ m^{-1} s^{-1} and the viscosity employed in the simulation is $\nu = 200$ m^2 s^{-1}. These values give a Reynolds number of Re $\sim$ 750 and a β parameter of $\hat{\beta} \sim 300$, corresponding most closely to Figs. 8b and 8c. There are indeed many features in common between the character of the flow in these calculations and the circulation in the FRAM simulation, including the inertial jet upstream of Kerguelen Plateau, the attached streamlines downstream of the plateau, and the downstream standing Rossby waves. In an idealized study of Southern Ocean dynamics, using a two-layer model and similar values of $\hat{\beta}$ and Re, we obtain similar jets upstream of the seamount together with a upstream blocked region (Tansley and Marshall 2001). These circulations also bear some similarities to the simple models of Webb (1993) and Pedlosky et al. (1997).

5. Concluding remarks

In this manuscript, we have revisited the problem of eastward flow past a cylinder on a β plane. The solutions are dependent on two nondimensional parameters: the Reynolds number, Re, and a nondimensional β parameter, $\hat{\beta}$.

At larger values of $\hat{\beta}$, a blocked, stagnant region forms upstream of the cylinder, flanked by two inertial jets, in accord with previous studies. We suggest that the large $\hat{\beta}$ limit is relevant to the interaction of the Antarctic Circumpolar Current with topographic obstacles such as the Kerguelen Plateau.

However, at sufficiently high Reynolds number (Re $>$ 200) and moderate β parameter ($\hat{\beta} \sim$ 10–100), we obtain a new regime with two separated inertial jets *downstream* of the cylinder. The extended jets are maintained by the downstream Rossby waves that break to form a turbulent wake, giving a downscale cascade of vorticity and an upscale cascade of energy toward the Rhines scale. Through a series of numerical experi-

ments, we have demonstrated the relevance of this regime to the separation of a boundary current from a cape. The implications are that Gulf Stream separation at Cape Hatteras is the consequence of *both* the high Reynolds number in the ocean and the moderate β parameter associated with the curvature of the coastline at Cape Hatteras. A more general analysis of the roles of the β effect and coastline curvature in boundary current separation at high Reynolds number is pursued in Marshall and Tansley (2001). Our results also suggest that geostrophic eddy fluxes are essential in maintaining a tight separated jet.

An important corollary of our study is that higher-resolution ocean models can obtain significantly improved boundary current separation behavior through the use of biharmonic dissipation. This allows the Laplacian dissipation to be reduced or indeed removed altogether, thereby raising the effective Reynolds number in the model calculations.

In this paper we have restricted our attention to barotropic results. Stratification will introduce an additional spatial scale—the deformation radius. Blanchonette (1998) has performed a series of numerical calculations for two-layer flow past a cylinder on an f plane. He finds that the zonal extent of the separated region downstream of the cylinder differs between the two layers, due to the ''effective β'' introduced by the sloping layer interface. Some preliminary results for two-layer flow past a cylinder on a β plane have also been obtained by Merkine and Brevdo (1986) in the limit of low $\hat{\beta}$. We are not aware of any studies to date addressing stratified flow past a cylinder at larger values of $\hat{\beta}$. Nevertheless, we believe that the simple barotropic calculations reported here are successful in describing several aspects of the observed and modeled circulations of the Gulf Stream and Antarctic Circumpolar Current.

Acknowledgments. The original idea for this work stemmed from a conversation with Raymond Hide. We wish to thank two anonymous reviewers whose comments led to a greatly improved manuscript. Numerous helpful conversations with Maarten Ambaum are also gratefully acknowledged. Financial support was provided by the U.K. Natural Environment Research Council (GR3/10157 and GR3/12861).

REFERENCES

Adcroft, A., and D. Marshall, 1998: How slippery are piecewise-constant coastlines in numerical ocean models? *Tellus,* **50A,** 95–108.

Batchelor, G. K., 1967: *An Introduction to Fluid Dynamics.* Cambridge University Press, 615 pp.

Blanchonette, P., 1998: Two-layer flow past a cylinder in a rotating frame. *J. Fluid Mech.,* **371,** 301–318.

Boyer, D. L., 1970: Flow past a right circular cylinder in a rotating frame. *J. Basic Eng.,* **92,** 430–436.

——, and P. A. Davies, 1982: Flow past a circular cylinder on a β-plane. *Philos. Trans. Roy. Soc. London,* **306A,** 533–556.

Dengg, J., 1993: The problem of Gulf Stream: A barotropic approach. *J. Phys. Oceanogr.,* **23,** 2182–2200.

——, A. Beckmann, and R. Gerdes, 1996: The Gulf Stream separation problem. *The Warmwatersphere of the North Atlantic,* W. Kraus, Ed., Gebruder Borntrager, 253–289.

Fofonoff, N. P., 1954: Steady flow in a frictionless homogeneous ocean. *J. Mar. Res.,* **13,** 254–262.

Foster, M. R., 1985: Delayed separation in eastward, rotating flow on a β-plane. *J. Fluid Mech.,* **155,** 59–75.

Hide, R., and L. M. Hocking, 1979: On detached shear layers and western boundary currents in a rotating homogeneous liquid. *Geophys. Astrophys. Fluid Dyn.,* **14,** 19–43.

Long, R. R., 1955: Some aspects of the flow of stratified fluids. III: Continuous density gradients. *Tellus,* **7,** 341–357.

Marshall, D. P., and C. E. Tansley 2001: An implicit formula for boundary current separation. *J. Phys. Oceanogr.,* **31,** 1633–1638.

Merkine, L. O., 1980: Flow separation on a β-plane. *J. Fluid Mech.,* **99,** 399–409.

——, and A. Solan, 1979: The separation of flow past a cylinder in a rotating system. *J. Fluid Mech.,* **92,** 381–392.

——, and L. Brevdo, 1986: Boundary layer separation of a two-layer rotating flow on a β-plane. *J. Fluid Mech.,* **167,** 31–48.

Moore, D. W., 1963: Rossby waves in ocean circulation. *Deep-Sea Res.,* **10,** 735–747.

Munk, W. H., 1950: On the wind-driven circulation. *J. Meteor.,* **7,** 79–93.

Page, M. A., and E. R. Johnson, 1990: Flow past cylindrical obstacles on a beta-plane. *J. Fluid Mech.,* **221,** 349–382.

Paiva, A. M., J. T. Hargrove, E. P. Chassignet, and R. Bleck, 1999: Turbulent behavior of a fine-mesh (1/12°) numerical simulation of the North Atlantic. *J. Mar. Syst.,* **21,** 307–320.

Pedlosky, J., 1987: *Geophysical Fluid Dynamics.* Springer-Verlag, 710 pp.

——, L. J. Pratt, M. A. Spall, and K. R. Helfrich, 1997: Circulation around islands and ridges. *J. Mar. Res.,* **55,** 1199–1251.

Rhines, P. B., 1975: Waves and turbulence on a beta-plane. *J. Fluid Mech.,* **69,** 417–433.

Smith, R. D., M. E. Maltrud, F. O. Bryan, and M. W. Hecht, 2000: Numerical simulation of the North Atlantic Ocean at 1/10°. *J. Phys. Oceanogr.,* **30,** 1532–1561.

Tansley, C. E., and D. P. Marshall, 2001: On the dynamics of wind-driven circumpolar currents. *J. Phys. Oceanogr.,* **31,** 3258–3273.

Van Dyke, M., 1982. *An Album of Fluid Motion.* Parabolic Press, 176 pp.

Webb, D. J., 1993: A simple model of the effect of the Kerguelen Plateau on the strength of the Antarctic Circumpolar Current. *Geophys. Astrophys. Fluid Dyn.,* **70,** 57–84.

——, P. D. Killworth, A. C. Coward, and S. R. Thompson, 1991. *The FRAM Atlas of the Southern Ocean.* U.K. Natural Environment Research Council, 67 pp.

White, W. B., 1971: A Rossby wake due to an island in an eastward current. *J. Phys. Oceanogr.,* **1,** 161–168.

Williams, G. P., 1978: Planetary circulations: I. Barotropic representation of Jovian and terrestrial turbulence. *J. Atmos. Sci.,* **35,** 1399–1426.